

# Filtered particle tracking for dispersed two-phase turbulent flows

By J. Pozorski †, S. V. Apte AND V. Raman

Turbulent particulate flows are considered in the Eulerian-Lagrangian approach where the large-eddy simulation of the carrier phase is coupled with the particle tracking. The issue addressed here is the impact of the subgrid scale turbulence on the statistics of particle motion, including preferential concentration. This is accomplished through *a priori* analysis of DNS data in the case of forced isotropic turbulence. A model for filtered particle tracking (FPT) is then proposed. The model aims to reconstruct the residual (subgrid scale) fluid velocity along particle trajectories. The computation results serve to appraise the model through comparisons with available DNS reference data on preferential concentrations for a selection of particle inertia parameters.

---

## 1. Introduction

Study of two-phase flows with dispersed droplets or solid particles constitutes an important activity in the realm of turbulence. There are variety of theoretical and modeling issues regarding this class of flows, both in the two-fluid and the trajectory approach (e.g., Simonin 1996; Minier & Peirano 2001). Practical applications involve environmental studies, chemical and process engineering, as well as power engineering, including wet steam flows and combustion of solid or liquid fossil fuels. A relevant industrial example is fuel injection in Diesel engine or a gas turbine combustor where the dispersed phase is present in the form of small droplets (Apte *et al.* 2003). In the paper, the dispersed phase will be assumed dilute; consequently, the one-way momentum coupling is adequate and particle collisions can safely be neglected. Yet, for a sufficiently high load of the dispersed phase, the two-way coupling needs to be accounted for in the momentum and energy equations; moreover, for high particle number densities, the interparticle collisions will affect their dynamics. Additional complexity to the physical picture will be added through the interphase mass and energy transfer in the case of evaporating droplets or volatilizing solid particles. Here, we concentrate on the dynamical aspects only, and precisely on the impact of turbulence on the statistics of the dispersed phase.

The Lagrangian stochastic approach has initially been proposed in its natural context for modeling and prediction of turbulent diffusion and dispersion. In the framework of statistical RANS (Reynolds-averaged Navier-Stokes) description of turbulence, various random walk models for the diffusion of fluid particles and the dispersion of solid particles in two-phase flows have been proposed since then, cf. Stock (1996), Pozorski & Minier (1998), Mashayek & Pandya (2003) and references therein. Following rapid progress in large eddy simulation (LES), the method has also been used with success to compute two-phase dispersed flows. The feasibility of LES to study preferential concentration of particles by turbulence (Wang & Squires 1996) and to compute flows with two-way momentum coupling (Boivin *et al.* 2000) has been reported.

† Institute of Fluid-Flow Machinery, Polish Academy of Sciences, Gdańsk, Poland

Generally speaking, some terms in the filtered LES evolution equations have to be modeled altogether, because relevant physical processes occur at unresolved scales; an example is the source term, due to chemical reactions, in mass and energy balance equations. Some other are partly resolved source terms due to the presence of particles: mass transport (evaporation/condensation), momentum coupling, and energy balance (heating, latent heat of evaporation). The issue of residual (unresolved, subgrid scale) velocity field and its influence on the statistics of particle motion and their preferential concentration has received only limited attention in the literature. It is revisited here with *a priori* tests using filtered DNS velocity fields.

The first aim of the paper is to study the impact of LES filtering on the particulate phase. It will be shown to be non-negligible for a sufficiently coarse LES mesh (judged by a residual kinetic energy content). A quantitative assessment of this effect is accomplished through the statistics of preferential particle concentration: the probability distribution of particle number density and the radial distribution function of the interparticle distance. The second aim of the paper is to develop a filtered particle tracking (FPT) model for the LES of the dispersed phase. The model is meant to reconstruct statistically the residual flow field along particle trajectories. First computation results are reported for the forced isotropic turbulence case.

## 2. Turbulent dispersion of particles

To determine the evolution of a set of non-interacting solid particles in turbulent flow, particle location  $\mathbf{x}_p$  and its velocity  $\mathbf{U}_p$  should be known. Another variable of importance for further considerations is the fluid velocity  $\mathbf{U}^*$  “seen” or sampled by the particle as it moves across the flow. In terms of the instantaneous Eulerian velocity field  $\mathbf{U}(\mathbf{x}, t)$  of the carrier (fluid) phase, we have  $\mathbf{U}^* = \mathbf{U}(\mathbf{x}_p, t)$ . Respective governing equations for particles are:

$$\frac{d\mathbf{x}_p}{dt} = \mathbf{U}_p, \quad (2.1)$$

$$\frac{d\mathbf{U}_p}{dt} = \frac{\mathbf{U}^* - \mathbf{U}_p}{\tau_p} + \mathbf{g}. \quad (2.2)$$

In general cases (Maxey & Riley 1983), the particle equation of motion (2.2) includes the pressure-gradient, drag, added-mass and Basset forces. Yet, for particles much heavier than the carrier fluid,  $\rho_p \gg \rho_f$  ( $\rho_f$  and  $\rho_p$  stand for fluid and particle densities), an acceptable approximation is to retain only the aerodynamic drag and external force terms  $\mathbf{g}$  (if relevant). The drag term is written using the particle relaxation time  $\tau_p$ .

Obviously, modeling of the fluid velocities sampled by particles is no longer needed when the carrier phase is fully resolved, possibly with source terms that represent the exchange of mass, momentum, and energy between the particles and the flow. This is the DNS with particle tracking where  $\mathbf{U}^*$  is simply the instantaneous fluid velocity interpolated at the point-particle location. Since the number of degrees of freedom in turbulent flows scales as  $\text{Re}^{9/4}$ , this approach is feasible only for simple flow cases at relatively small  $\text{Re}$ . Nevertheless, the DNS studies are extremely valuable for model testing, as evidenced in the following sections: preferential concentration patterns, first observed in experimental studies, are investigated (Sec. 3.3); the impact of filtering on particle statistics is assessed (Sec. 3.4). For a finite-size particle (comparable to the Kolmogorov scale  $\eta$  or larger), its dynamics, fluctuating lift and drag forces can be computed from “true DNS” studies (Bagchi & Balachandar 2003; Burton & Eaton 2003).

Despite the growing importance of DNS, a reduced (or contracted) description involving far less degrees of freedom is still used for practical, “real-life” flow cases. In particular, RANS remains a standard engineering approach. One of the difficult modeling aspects of turbulent dispersion in RANS is the account of the fluid velocity statistics seen along the solid particle trajectories. They unavoidably differ from the “pure” Lagrangian statistics because of the particle inertia and the external force (such as gravity) effects. Stochastic models based on the Langevin equation have been proposed to account for these effects (Pozorski & Minier 1998; Minier *et al.* 2004). Alternatively, the PDF formalism, initially developed in turbulence modeling (cf. Pope 2000), and particularly useful in turbulent combustion (Fox 2003), has been extended to turbulent dispersion issues, starting with the kinetic equation of Reeks (1992) and further developed by Pozorski & Minier (1999).

In general terms, a physically-sound reconstruction of instantaneous fluid velocity “seen” by the particles  $\mathbf{U}^*$  has to be performed out of limited information available (such as the fluid mean velocity  $\langle \mathbf{U} \rangle$  or its turbulent kinetic energy). A classical approach goes through the decomposition  $\mathbf{U}^* = \langle \mathbf{U} \rangle + \mathbf{u}^*$  with the mean fluid velocity at the particle location,  $\langle \mathbf{U} \rangle(\mathbf{x}_p, t)$ , determined from the Eulerian RANS solver for the carrier phase. Various stochastic models have been proposed to represent the fluctuating fluid velocity  $\mathbf{u}^*$  sampled by particles. They often are extensions of fluid diffusion models, developed in the context of environmental and atmospheric studies, but can suffer from spurious drifts if improperly devised (MacInnes & Bracco 1992). A sound alternative seems to be a stochastic model for  $\mathbf{U}^*$  (Pozorski & Minier 1999; Minier *et al.* 2004).

In the context of RANS, there are no instantaneous flow structures resolved; consequently, there is no preferential concentration (which, by definition, denotes correlation of particle locations with certain flow structures). In RANS of non-homogeneous turbulence, spatial gradients of particle number density can develop (even for initially uniform particle distribution) because of the so-called turbophoresis effect. It consists in the net particle displacement in the direction of decreasing turbulence intensity (for  $\rho_p > \rho_f$ ).

In LES, the resolved (large-scale) part of the instantaneous flow field can readily be interpolated to particle locations. The major issue is now to determine whether the remaining (residual or subgrid-scale) part of the flow velocity field can have a noticeable influence on the particulate phase. In most studies reported so far, this influence has been neglected and justified by a low residual energy content. A LES study of particle-laden channel flow was reported by Wang & Squires (1996). Analysis of their data (Fig. 4 there) shows that the ratio of  $k_{\text{sg}}$  to  $\bar{u}^2$  remains small throughout the viscous sublayer (roughly 10%). Armenio *et al.* (1999) computed channel flow with the one-way momentum coupling. Particles were tracked in a fully-resolved (DNS) velocity field and in filtered fields where up to 20% of the turbulent kinetic energy remained unresolved depending on the filter size; however, there was no filtering in the wall-normal direction. They performed then a corresponding LES with the same filter width. In all cases, the r.m.s. particle dispersion was found to be only slightly affected by the incomplete resolution.

Okong’o & Bellan (2004) performed an *a priori* analysis of a dispersed two-phase flow. They distinguished four possibilities for the reconstruction of SGS fluid velocities “seen”: ideal model (velocity  $U_i$  from DNS data), baseline model (velocity  $\tilde{U}_i$  from LES), random model (velocity reconstructed as  $\tilde{U}_i + \sigma \xi_i$  where  $\xi_i$  are Gaussian random numbers) and deterministic model (not explained here). The eddy life-time and interaction-time model known in RANS has been extended to LES by Oefelein (cf. Segura *et al.* 2004) and successfully applied to the channel flow. Also Sankaran & Menon (2002) proposed a simple FPT model, yet its impact on final LES results has not been reported.

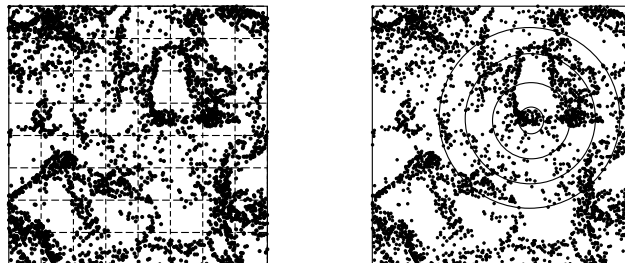


FIGURE 1. Computing the particle number density and the radial distribution function.

### 3. Preferential concentration of particles in turbulent flows

#### 3.1. Effect of turbulent structures on particles

Instantaneous structures of the turbulent velocity field influence the motion of heavy particles (droplets), depending on their inertia. A convenient definition of the Stokes number goes here through the normalization with the Kolmogorov time scale:  $St = \tau_p / \tau_\eta$ . Particles of  $St = \mathcal{O}(1)$  tend to correlate with certain eddy structures and this leads to the effect of preferential concentration, i.e. accumulation of particles in flow regions of low vorticity and high rate of strain (streams, convergence zones); cf. Eaton & Fessler (1994) for review. Studies reported in the literature include DNS of isotropic turbulence (Squires & Eaton 1991; Wang & Maxey 1993) as well as LES (Wang & Squires 1996).

The preferential concentration changes the physical picture of particulate flows in several ways: it affects the particle deposition on walls (Uijtewaal & Oliemans 1996); it leads to an increase of interparticle collision rates and, possibly, coalescence in a dense two-phase flow regime (Reade & Collins 2000); it influences the particle settling velocity in an external (gravity) field (Wang & Maxey 1993).

#### 3.2. Quantifying preferential concentration

Various measures of preferential concentration have been established in the literature, cf. Hogan & Cuzzi (2001) for a comparative study and sensitivity tests with respect to the Reynolds number and bin size. Preferential concentration can be quantified by the PDF of particle number density based on bin counting, cf. Fig. 1(a). The distribution of particle number  $n = N_{PC}$  per bin (or per cell),  $f_B(n)$ , will depend on  $St$  and on the bin size. For a random (uncorrelated) distribution of particles in the domain, the PDF is the discrete Poisson distribution,  $f_P(n)$ , with the parameter being the mean of the number density (exactly: the average number of particles per cell,  $\langle N_{PC} \rangle$ )

$$f_P(n) = \frac{e^{-\lambda}}{n!} \lambda^n, \quad \lambda = \langle N_{PC} \rangle. \quad (3.1)$$

A natural measure of the non-uniform particle concentration is the deviation of the actual (measured) number density from the random one (Wang & Maxey 1993):

$$\tilde{D} = \sum_{n=1}^{\infty} [f_B(n) - f_P(n)]^2. \quad (3.2)$$

Another measure of preferential concentration is

$$D = \frac{s - s_P}{\lambda} \quad (3.3)$$

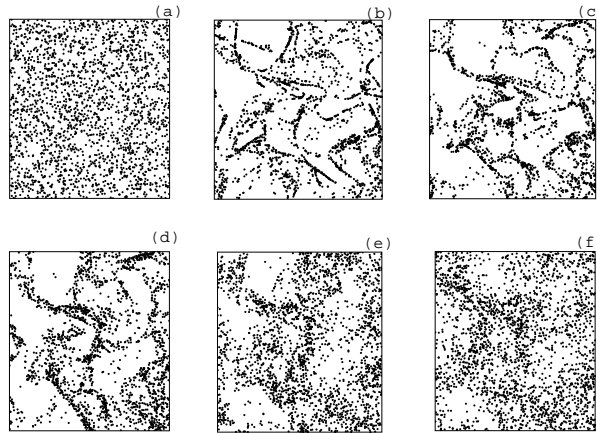


FIGURE 2. Snapshots of particle positions from DNS; runs with various values of the particle inertia parameter: a)  $St = 0.01$ , b)  $St = 0.2$ , c)  $St = 0.7$ , d)  $St = 1$ , e)  $St = 2$ , f)  $St = 4$ .

where  $s$  is the standard deviation of the actual number of particles per bin, and  $s_P = \lambda^{1/2}$  is the standard deviation of the corresponding Poisson distribution; normally,  $D \geq 0$ .

Yet another possibility to quantify the non-uniform particle concentration comes from the two-point spatial distribution function. For a statistically isotropic and homogeneous system of particles, Reade & Collins (2000) introduced the radial distribution function (RDF) of particle location,  $g(r)$ , derived from the two-point RDF  $f^{(2)}(r)$  where  $r = |\mathbf{x}_2 - \mathbf{x}_1|$  for particles located at points  $\mathbf{x}_2$  and  $\mathbf{x}_1$ , cf. Fig. 1(b). Basically,  $g(r)dr$  is the number of particles located in a spherical cell  $(r, r+dr)$  around  $\mathbf{x}_1$ , divided by the expected number of particles if their distribution were uniform, and averaged over first-particle locations  $\mathbf{x}_1$ . The RDF is close to unity for a uniformly distributed particle system. Moreover,  $g(r)$  can provide a clear estimation of the characteristic length scale of preferential concentration (if any).

### 3.3. DNS of particle-laden, forced isotropic turbulence

The DNS of forced isotropic turbulence at  $Re_\lambda \approx 40$  has been undertaken on a  $96^3$  grid. The particle tracking has been performed in the DNS velocity field with the assumption of one-way momentum coupling. This has been done for a selection of particle inertia parameters (the Stokes number). The resulting snapshots of particle locations are shown in Fig. 2. As readily noticed, the preferential concentration of particles is most visible for  $0.2 < St < 2$ , in agreement with earlier observations of Squires & Eaton (1991).

The bin counting has been applied to particle locations in 3D with the bin size varying from the cell size of the DNS ( $\Delta_{\text{bin}} = \Delta$ ) up to 1/6 of the domain size ( $\Delta_{\text{bin}} = 32\Delta$ ). As evidenced by the profiles of  $f_B$  in Fig. 3, the random particle pattern (the Poisson distribution) is noticed for the smallest particles tracked ( $St=0.01$ ) for all bin sizes. Also for the largest particles ( $St=4$ ) the pattern is basically random, specially for smaller bin sizes. Intermediate-size particles tend to deviate most from the random distribution. As noticed from Fig. 3(d), the limit behavior for large  $\langle N_{PC} \rangle$  (larger bins) is well reproduced, i.e. the Poisson distribution, Eq. (3.1), tends to the Gaussian PDF,  $\mathcal{N}(\lambda, \lambda^{1/2})$ .

For particles in isotropic turbulence,  $\tilde{D}$  computed from Eq. (3.2) is shown in Fig. 4(a); the profile of  $D$ , Eq. (3.3), is shown in Fig. 4(b). Both confirm the visual impression from Fig. 2 that the maximum of preferential concentration occurs for particles of  $St = \mathcal{O}(1)$ .

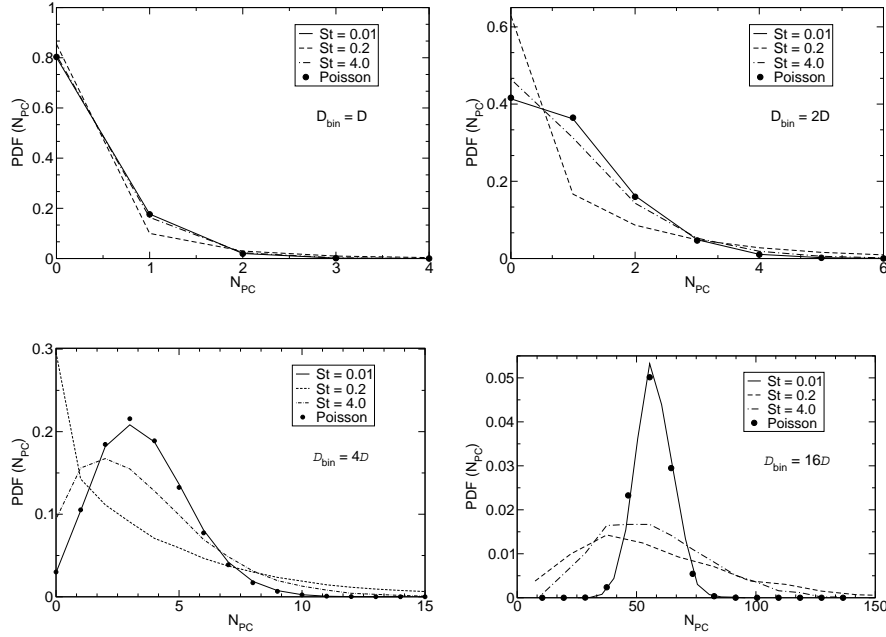


FIGURE 3. PDF of particle number density for different bin sizes: a)  $\Delta$ , b)  $2\Delta$ , c)  $4\Delta$ , d)  $16\Delta$ .

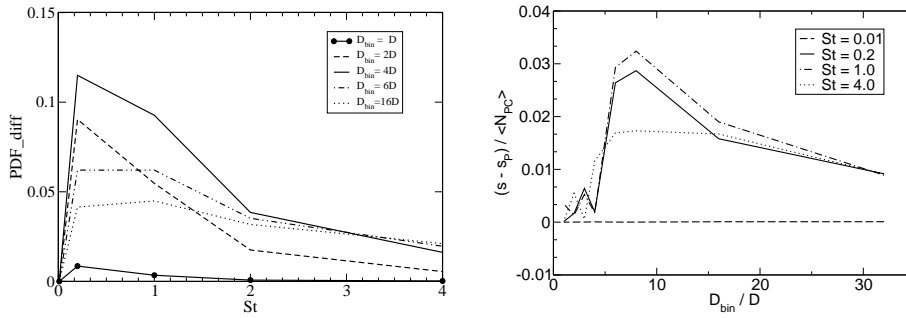


FIGURE 4. Measures of preferential concentration: a) difference of PDFs of particle number density (actual and Poisson), Eq. (3.2); b) difference of standard deviations, Eq. (3.3).

To illustrate how the RDF  $g(r)$  works in practice, we considered three simple, predetermined particle patterns in 3D (Fig. 5): random, ordered with a short length scale  $l$ , and ordered at a larger scale  $L$  (resulting in a checkered pattern). As quantified by the RDF in Fig. 6(a), neither random nor short-scale ordered pattern ( $l < \Delta_{\text{bin}}$ ) exhibit any preferential concentration. For the checkered pattern ( $L > \Delta_{\text{bin}}$ ), the non-uniformities are reflected in the RDF; moreover, the characteristic scale of the pattern ( $\sim L$ ) is retrieved from the plot. Then, we repeated the procedure for the particles moving in the DNS flow field. The plots in Fig. 6(b) show a departure from the uniform (random) distribution of particle locations in space, most pronounced for  $0.2 < St < 2$ . The characteristic length scale of the pattern is about  $10\eta$ .

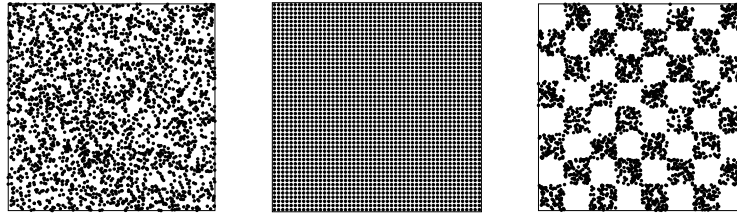
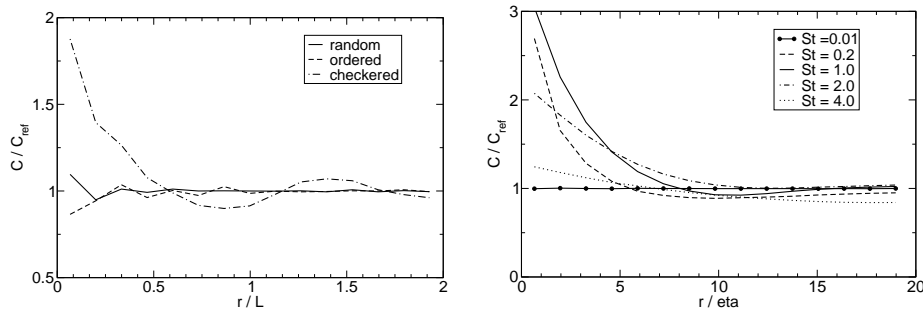
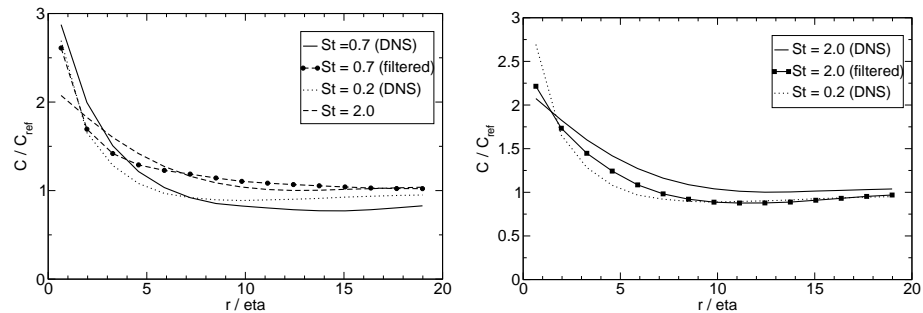


FIGURE 5. Tests for various particle arrangements: a) random, b) ordered, c) checkered.


 FIGURE 6. Particle radial distribution functions: a) pre-arranged pattern, b) DNS at  $St = 1$ .

 FIGURE 7. RDF of particles tracked in a filtered DNS field. (a)  $St = 0.7$ ; (b)  $St = 2.0$ .

### 3.4. A priori tests of preferential concentration: particle tracking in filtered DNS field

To the best of the authors knowledge, the effect of LES filtering on preferential particle concentration has not been studied so far. An interesting finding results from an *a priori* test as follows. The instantaneous DNS velocity field has been filtered so that  $k_{\text{filtered}} = 0.65k_{\text{DNS}}$ . Then, the particles have been tracked in a smoothed velocity field. To determine the impact of smoothing on preferential concentration, the statistics of the particle number density in the physical space have been gathered. The pattern of preferential concentration is indeed modified by filtering. As noticed from the computed RDF of particle locations (Fig. 7), in filtered velocity field particles behave as though their effective Stokes number were larger; yet, short-scale correlations remain strong. This gives us some hint as to the construction of a FPT model. The snapshots of particle locations moving in the smoothed (LES-like) velocity field are shown in Figs. 8(b) and 9(b).

#### 4. Reconstructing residual fluid velocity field along particle paths

##### 4.1. Reasons behind FPT modeling

In LES, by definition of the method, a major part of the turbulent kinetic energy should be resolved (say, 80%, Pope 2000). Yet, this can be estimated only in simple cases where there is a DNS study at hand. For practically-relevant computations, the resolution often varies in space. The LES is known to face particular difficulties in wall-bounded flows, since the complete near-wall resolution becomes costly as the number of grid nodes scales roughly as  $\text{Re}^{1.8}$  (cf. Pope 2000) and wall-modeling (or hybrid RANS/LES approach) is preferred. Also in this case, the SGS energy content may be considerable.

Regarding the LES of two-phase dispersed flows, several new issues appear. A concern about LES with the two-way coupling (of mass, momentum, energy) relates to the modeling of carrier phase source terms due to particles. Another concern, of importance here, is the impact of unresolved (subgrid-scale) flow quantities on particles: their dispersion, preferential concentration, deposition on walls. It can vary depending on the particle inertia parameter. In particular, for evaporating spray flow, the droplets unavoidably enter the size range where there is an impact from the flow SGS. In a numerical study of near-wall turbulence, Uijttewaal & Oliemans (1996) pointed out to the significant deviation of their LES results on particle deposition on the wall with respect to reference data. The LES predicted the particle deposition coefficient to be one order of magnitude smaller than the value found in experiment and DNS. A probable reason was the insufficient resolution of near-wall eddies responsible for deposition of smaller particles, and a need of a model to account for subgrid scale effects on particles was suggested.

##### 4.2. Requirements for a FPT model

To specify criteria of a good SGS dispersion model, let us start from the well-established case of single-phase LES. Arguably, a sound model for the SGS stress should simulate the effects of small eddies without altering the motion at large-eddy scales. For particle-laden turbulent flows, but still with the one-way coupling of mass, momentum, and energy (i.e., no evaporation/condensation, light loading, no heat transfer), a pre-requisite for a good SGS dispersion model, suitable for FPT, is that particle characteristics should remain close to those from a fully-resolved computation. They include the statistics of instantaneous particle locations (preferential concentration, if any), averaged locations (e.g., the r.m.s. particle position in line-source dispersion, the concentration profile in jet or mixing layer), and velocities (turbulent kinetic energy, Lagrangian velocity autocorrelation).

The constraints to be satisfied by a FPT model are: (i) in the limit of fully-resolved computation (LES becomes then DNS,  $k_{\text{sg}} \rightarrow 0$ ), the model should have no effect on particle motion; (ii) in the limit of small particles ( $\tau_p/\tau_f \rightarrow 0$ ) the model should boil down to the prediction of fluid diffusion; the velocity filtered density function approach (VFDF) of Gicquel *et al.* (2002) may possibly serve as the limit case to compare with; (iii) in the limit of large particles ( $\tau_p/\tau_f \rightarrow \infty$ ) the model should have no short-time effect on particle motion; (iv) in the presence of external force field (gravity), the model should possibly take it into account; (v) in the limit of under-resolved velocity field (LES becomes then RANS,  $k_{\text{sg}} \rightarrow k$ ), the particle turbulent dispersion should be fully modeled; (vi) for pairs of neighboring particles (located within the same cell or closer to each other than  $\mathcal{O}(\Delta_f)$ ), the model should possibly account for relative dispersion effects.

Yet, we perceive the constraints (i)–(iii) as really important for FPT models in the context of LES. The effects of external fields (iv) are, apparently, not well known; the limit of RANS (v) is unlikely to be approached in real-life LES computations. Concerning



the relative dispersion issue (vi), it cannot be accounted for in the one-point approach that is of interest here because of computational efficiency.

An essential ingredient of FPT models is the residual kinetic energy,  $k_{\text{sg}}$  say. It determines the level of residual velocity fluctuations, also those “seen” by particles. In a particular test case considered here (forced isotropic turbulence),  $k_{\text{sg}}$  can readily be found from the DNS data (raw and filtered). In general case, the subgrid kinetic energy of the flow can be estimated from its transport equation. Wang & Squires (1996) and Sankaran & Menon (2002) recall the  $k_{\text{sg}}$  equation based on the Schumann non-equilibrium model.

#### 4.3. Simple FPT model for locally homogeneous and isotropic turbulence

A reasonable assumption about LES is to consider the residual turbulent motion as locally homogeneous and isotropic. Then, the fluid velocity “seen” by particles is computed as  $U_i^* = \tilde{U}_i(\mathbf{x}_p, t) + u_i^*$ , i.e. the sum of the filtered LES velocity  $\tilde{U}_i$  interpolated at the particle location and the residual velocity “seen” by the particle.

Crucial ingredients of an FTP model are the SGS turbulent kinetic energy of the fluid and a SGS time scale. By analogy to modeling turbulent diffusion of fluid elements in the context of statistical (RANS) description (Pozorski & Minier 1999), we assume that  $\mathbf{u}^*$  is governed by the Langevin equation

$$du_i^* = -\frac{u_i^*}{\tau_L^*} dt + \sqrt{\frac{2\sigma_{\text{sg}}^2}{\tau_L^*}} dW_i \quad (4.1)$$

where  $\sigma_{\text{sg}}$  and  $\tau_L^*$  stand for the respective velocity and time scales of residual motions “seen” by the particle; moreover, let  $\tau_{\text{sg}}$  denote the time scale of residual motions. They are estimated from

$$\sigma_{\text{sg}} = \sqrt{\frac{2}{3}k_{\text{sg}}}, \quad \tau_L^* = f(\tau_{\text{sg}}, \tau_p, \sigma_{\text{sg}}/g), \quad \tau_{\text{sg}} = C \frac{\Delta f}{\sqrt{\frac{2}{3}k_{\text{sg}}}}. \quad (4.2)$$

The model constant  $C = \mathcal{O}(1)$  accounts for the uncertainty concerning the time scale of the residual velocity autocorrelation. The prediction  $\tau_L^* = \tau_{\text{sg}}$  is expected to work well for small St (also in the limit case of fluid diffusion). For larger St, we tentatively propose an extension of the model for RANS particle dispersion (Pozorski & Minier 1999) drawing on the Csanady expressions to account for the crossing-trajectory effect. The time scale will now differ in the directions parallel and perpendicular to the relative velocity  $\tilde{\mathbf{U}} - \mathbf{U}_p$

$$\tau_{L,||}^* = \frac{\tau_{\text{sg}}}{\sqrt{1 + \beta^2 \xi^2}}, \quad \tau_{L,\perp}^* = \frac{\tau_{\text{sg}}}{\sqrt{1 + 4\beta^2 \xi^2}} \quad (4.3)$$

where  $\xi$  is the normalized drift velocity determined from  $\xi = |\tilde{\mathbf{U}} - \mathbf{U}_p|/\sigma_{\text{sg}}$ . In the context of RANS,  $\beta$  is the ratio of Lagrangian to Eulerian time scales  $\beta = T_L/T_E$ ; for SGS velocity field we assume  $\beta = 1$ .

In practical implementation, a discrete version of the model (unconditionally stable, first-order accuracy in time) becomes

$$u_i^{*(n+1)} = au_i^{*(n)} + b\xi_i \quad (4.4)$$

where  $\Delta t = t^{(n+1)} - t^{(n)}$  is the time interval and  $\xi_i$  are random numbers from the standard Gaussian distribution,  $\xi_i \in \mathcal{N}(0, 1)$ . The coefficients  $a$  and  $b$  are given by the explicit solution of the stochastic differential equation (SDE), Eq. (4.1), with frozen coefficients

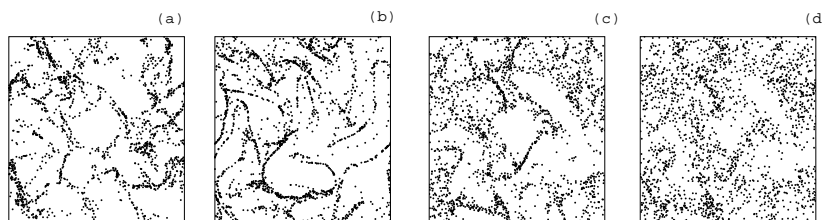


FIGURE 8. Snapshots of particle positions; runs for particles of  $St = 0.7$ . a) DNS; b) *a priori* LES with with no FPT model; c) *a priori* LES with FPT model and  $C=0$ ; d) with  $C=0.05$ .

over a time step  $\Delta t$ :

$$a = e^{-\Delta t/\tau_L^*}, \quad b = \sigma_{sg} \sqrt{1 - e^{-2\Delta t/\tau_L^*}}. \quad (4.5)$$

In the particular example of Eq. (4.1), which is a SDE with constant coefficients, the solution provided by Eqs. (4.4) and (4.5) is exact. However, the construction of higher-order numerical schemes for general (variable coefficients) SDEs remains an open issue.

Equation (4.4) can be further simplified to the Euler scheme

$$u_i^{*(n+1)} = \left(1 - \frac{\Delta t}{\tau_L^*}\right) u_i^{*(n)} + \sigma_{sg} \sqrt{\frac{2\Delta t}{\tau_L^*}} \xi_i. \quad (4.6)$$

Yet, in contrast to formulation (4.4)–(4.5), discretization (4.6) does impose a time step restriction  $\Delta t < \tau_L^*$  because of stability concerns.

It may be interesting to note that in the limit of  $\Delta t \gg \tau_L^*$  the scheme (4.4) boils down to generating a series of independent successive velocities  $\mathbf{u}^*$ , i.e.

$$\mathbf{u}^{*(n+1)} = \sigma_{sg} \boldsymbol{\xi}. \quad (4.7)$$

However, for a physically-consistent use of Eq. (4.7), it is imperative that the time intervals for generating a series of independent velocity realizations be  $2\tau_L^*$  in order to preserve the correlation time scale (cf. Pozorski & Minier 1998).

#### 4.4. First results of the FPT model

We have tested the FPT model (4.1) in *a priori* LES computations of forced isotropic turbulence for the same conditions as those described in Sec. 3.3. The computational results for two values of the Stokes number and some choices of the model constant are shown in Figs. 8 and 9. The impact of the residual velocity field, reconstructed in FPT, is readily noticed. As expected, the one-point stochastic model introduced here has a “randomizing” effect on particle locations. For particle sizes larger than that of maximum preferential concentration effect (roughly  $St \approx 1$  in our case) the randomizing effect of small scales is lost (the picture of preferential concentration becomes overly sharp), so the model is meant to restore it, cf. Fig. 9. In the case of smaller particles that are most influenced by smaller eddies and correlated on a shorter length scale, it is shown in Fig. 8 that the filtering does an inverse effect, i.e. it partly kills this short-scale preferential concentration (the picture of preferential concentration becomes somewhat “blurred”), so a potentially successful model for this case should rather be of an “antidiffusive” character (arguably, scale-similarity arguments can be used for its construction).

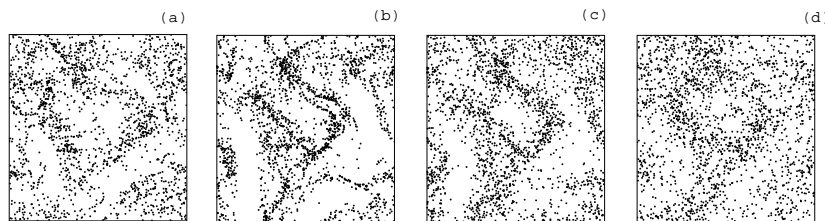


FIGURE 9. Snapshots of particle positions; runs for particles of  $St = 2$ . a) DNS; b) *a priori* LES with no FPT model; c) *a priori* LES with FPT model and  $C=0.05$ ; d) DNS for  $St = 4$ .

## 5. Conclusion and future plans

In the present paper, we have shown the impact of LES filtering on particle motion in turbulent flows. In particular, the particle preferential concentration patterns change. A stochastic model has been proposed to reconstruct the residual velocity field along particle trajectories. First results with the model seem encouraging. A lingering question as to FPT is that it is only a single-realization (one-particle) approach. The statistical interpretation of the model has to be thought over, also in the context of parcels (representing many solid particles). Further developments are warranted for more general flow fields. Arguably, an improved model should consist of a random ingredient (since the details of residual fluid motion are unknown) and possibly also of a deterministic ingredient, dependent on the structure of the resolved field and justified by the hope that the largest unresolved scales are in a sense similar to resolved ones.

A further-term objective is to unify the LES/FPT approach for the dispersed flows, presented above, with the LES/FDF approach for flows with scalars, possibly reactive, developed by Colucci *et al.* (1998). This should ultimately provide a physically-sound, yet efficient, tool for the computation of dispersed turbulent two-phase flows with chemical reactions (spray combustion). In this formulation, the vector of stochastic variables associated with particles will include  $\mathbf{x}_p$ ,  $\mathbf{U}_p$ ,  $\mathbf{U}^*$ ,  $d_p$ ,  $T_p$ , and chemistry-related quantities.

## Acknowledgments

We wish to thank Frank Ham and Olivier Desjardins for their assistance. We are grateful to Professor John Eaton for his insightful comments on the manuscript.

## REFERENCES

- APTE, S. V., MAHESH, K., MOIN, P. & OEFELEIN, J. C. 2003 LES of swirling particle-laden flows in a coaxial-jet combustor. *Int. J. Multiphase Flow* **29**, 1311–1331.
- ARMENIO, V., PIOMELLI, U. & FIOROTTO, V. 1999 Effect of the subgrid scales on particle motion. *Phys. Fluids* **11**, 3030–3042.
- BAGCHI, P. & BALACHANDAR, S. 2003 Effect of turbulence on the drag and lift of a particle. *Phys. Fluids* **15**, 3496–3513.
- BOIVIN, M., SIMONIN, O. & SQUIRES, K. D. 2000 On the prediction of gas-solid flows with two-way coupling using large eddy simulation. *Phys. Fluids* **12**, 2080–2090.
- BURTON, T. M. & EATON, J. K. 2003 Fully resolved simulations of particle-turbulence interaction. *Rep. No. TSD-151*, Dept. of Mech. Engng., Stanford University.
- COLUCCI, P. J., JABERI, F. A., GIVI, P. & POPE, S. B. 1998 Filtered density function for large eddy simulation of turbulent reacting flows. *Phys. Fluids* **10**, 499–515.

- EATON, J. & FESSLER, J. R. 1994 Preferential concentration of particles by turbulence. *Int. J. Multiphase Flow* **20**, Suppl., 169–209.
- FOX, R. O. 2003 *Computational Models for Turbulent Reacting Flows*. Cambridge University Press.
- GICQUEL, L. Y. M., GIVI, P., JABERI, F. A. & POPE, S. B. 2002 Velocity filtered density function for LES of turbulent flows. *Phys. Fluids* **14**, 1196–1213.
- HOGAN, R. C. & CUZZI, J. N. 2001 Stokes and Reynolds number dependence on preferential particle concentration in simulated 3D turbulence. *Phys. Fluids* **13**, 2938–2945.
- MACINNES, J. M. & BRACCO, F. V. 1992 Stochastic particle dispersion modeling and the tracer-particle limit. *Phys. Fluids A* **4**, 2809–2824.
- MASHAYEK, F. & PANDYA, R. V. R. 2003 Analytical description of two-phase turbulent flows. *Prog. Energy Combust. Sci.* **29**, 329–378.
- MAXEY, M. R. & RILEY, J. J. 1983 Equation of motion for a small rigid sphere in a nonuniform flow. *Phys. Fluids* **26**, 883–889.
- MINIER, J. P. & PEIRANO, E. 2001 The PDF approach to turbulent polydispersed two-phase flows. *Phys. Reports* **352**, 1–214.
- MINIER, J. P., PEIRANO, E. & CHIBBARO, S. 2004 PDF model based on Langevin equation for polydispersed two-phase flows applied to a bluff-body gas-solid flow. *Phys. Fluids* **16**, 2419–2431.
- OKONG'O, N. A. & BELLAN, J. 2004 Consistent large-eddy simulation of a temporal mixing layer laden with evaporating drops. Part 1. Direct numerical simulation, formulation and *a priori* analysis. *J. Fluid Mech.* **499**, 1–47.
- POPE, S. B. 2000 *Turbulent Flows*. Cambridge University Press.
- POZORSKI, J. & MINIER, J. P. 1998 On the Lagrangian turbulent dispersion models based on the Langevin equation. *Int. J. Multiphase Flow* **24**, 913–945.
- POZORSKI, J. & MINIER, J. P. 1999 PDF modeling of dispersed two-phase turbulent flows. *Phys. Rev. E* **59**, 855–863.
- READE, W. C. & COLLINS, L. R. 2000 Effect of preferential concentration on turbulent collision rates. *Phys. Fluids* **12**, 2530–2540.
- REEKS, M. W. 1992 On the continuum equations for dispersed particles in nonuniform flows. *Phys. Fluids A* **4**, 1290–1303.
- SANKARAN, V. & MENON, S. 2002 LES of spray combustion in swirling flows. *J. Turbulence* **3**, art. no. 011.
- SEGURA, J. C., EATON, J. K. & OEFELIN, J. C. 2004 Predictive capabilities of particle-laden LES. *Rep. No. TSD-156*, Dept. of Mech. Engng., Stanford University.
- SIMONIN, O. 1996 Eulerian numerical approach for prediction of gas-solid turbulent two-phase flows. *Von Karman Institute Lecture Series*, Rhode-St-Genèse, Belgium.
- SQUIRES, K. D. & EATON, J. K. 1991 Preferential concentration of particles by turbulence. *Phys. Fluids A* **3**, 1169–1178.
- STOCK, D. E. 1996 Particle dispersion in flowing gases. *J. Fluids Engng.* **118**, 4–17.
- UIJTTEWAALL, W. S. J. & OLIEMANS, R. V. A. 1996 Particle dispersion and deposition in DNS and LES of vertical pipe flows. *Phys. Fluids* **8**, 2590–2604.
- WANG, L. P. & MAXEY, M. R. 1993 Settling velocity and concentration distribution of heavy particles in homogeneous isotropic turbulence. *J. Fluid Mech.* **256**, 27–68.
- WANG, Q. & SQUIRES, K. D. 1996 Large eddy simulation of particle-laden turbulent channel flow. *Phys. Fluids* **8**, 1207–1223.